Fluctuations of the Dynamic Topography in the Pacific Ocean[1]

KLAUS WYRTKI

Department of Oceanography, University of Hawaii, Honolulu 96822

(Manuscript received 26 September 1974, in revised form 3 February 1975)

ABSTRACT

The dynamic topography of the Pacific Ocean has been mapped and its mean annual and random variability has been investigated using approximately 66,600 hydrographic stations. Largest annual fluctuations are associated with the equatorial current system and are probably due to vertical displacements of the thermocline in response to the changing wind field. In the subtropical gyres and in higher latitudes, dynamic topography varies seasonally in response to the annual cycle of surface layer temperature, but the pattern of dynamic height does not change much between summer and winter. In the western portion of the North Pacific anticyclonic gyre, a U-shaped ridge is developed with its open end pointing east, which separates the western boundary current from the interior of the gyre and links the north equatorial ridge with a ridge at the right flank of the Kuroshio. The variability of dynamic height given by its standard deviation increases from east to west across the Pacific Ocean. Most of this variability is due to fluctuations in the position of currents, their meandering, and the presence of eddies.

1. Introduction

The dynamic topography of the sea surface relative to a deeper reference level is a good measure of the circulation in the surface layer of the ocean, as shown by Reid (1961) on the example of the Pacific Ocean. With increasing interest in the fluctuations of ocean circulation and an increasing data base, it becomes desirable to investigate the changes of dynamic topography throughout the year and its variability, regular or random. The reasons for this investigation are all related to the North Pacific Experiment (NORPAX), during which we plan to analyze the large-scale, long-range interactions of the ocean-atmosphere system. This analysis will also be useful in studies of the relationship between fluctuations of observed sea level and ocean circulation, such as those already begun by Wyrtki (1974a, b). Finally, we intend to investigate the possibility of using temperature profiles from expendable bathythermographs (XBT) in conjunction with average temperature-salinity curves to determine the dynamic topography for quasi-synoptic situations (Emery, 1975).

The variations of dynamic topography fall naturally into two groups, regular and random. The mean annual variation is chiefly caused by the annual cycles of the thermal structure associated with the annual heating and cooling cycle and the mean annual changes of the large wind systems. The random variability is due to the meandering of currents, the presence of eddies, and internal waves and tides. In this study I wish to analyze existing hydrographic data in order to document the distribution of variability of dynamic topography in the Pacific Ocean.

2. Data and data processing

The National Oceanographic Data Center (NODC) provided dynamic height computations for all hydrographic stations in the Pacific Ocean that had data to at least 500 m depth and were contained in their Oceanographic Station Data File as of April 1974. The computations were made in the manner outlined in the *User's Guide to NODC's Data Services* (NOAA, 1974). Data were received from 66,673 stations. Unfortunately, this data file does not contain observations made with temperature-salinity-depth recorders, which in recent years have contributed significant amounts of oceanographic data. Only the STD data resulting from the EASTROPAC Expedition in 1967–68 are included; these were given to us through the courtesy of Dr. M. Tsuchiya of the Scripps Institution of Oceanography, who has discussed the geostrophic flow patterns during the EASTROPAC Expedition (Tsuchiya, 1974).

The values of dynamic height relative to 1000 db calculated for individual stations were averaged for areas of 2° of latitude and longitude and for bimonthly periods, and standard deviations were computed. The derived values were computer-plotted in the form of maps, and were contoured by hand. Only a few obviously wrong values were deleted in this process. The contoured maps were then transferred to an equal area projection, the same as used by Reid (1961). Maps were prepared relative to 500 and 1000 db for each

[1] Hawaii Institute of Geophysics Contribution No. 670.

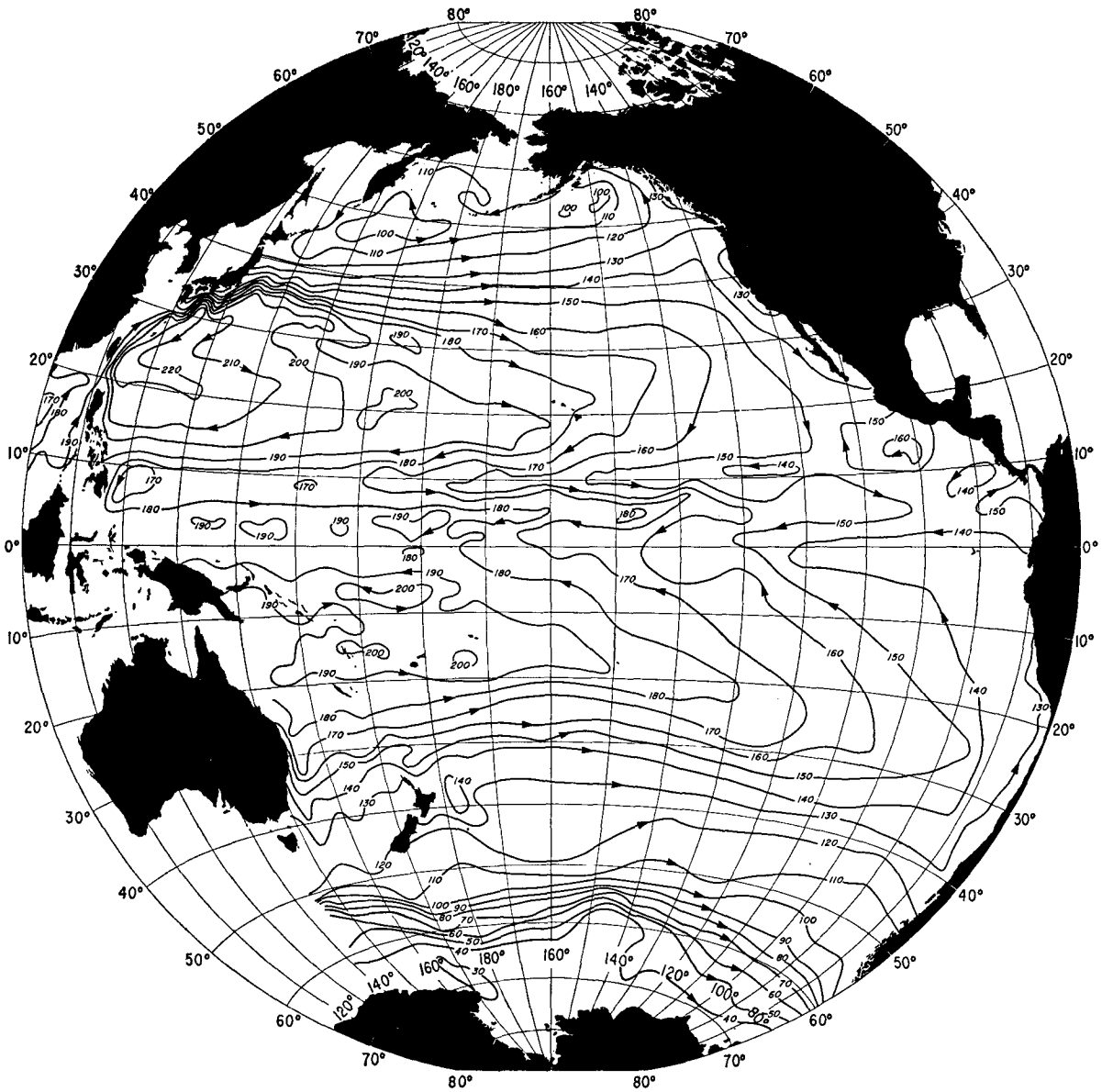

FIG. 1. Mean annual dynamic topography (dyn-cm) of the sea surface relative to 1000 db: 36,356 observations.

bimonthly period and for the annual mean, as well as for surface topography relative to 3000 db, for 500 db relative to 1000 db, and for 1000 db relative to 2000 db, but only a few are shown here. The others have been published in a technical report (Wyrtki, 1974c).

3. The mean annual dynamic topography

While the general pattern of dynamic height on our map of the mean annual dynamic topography (Fig. 1) is quite similar to that shown by Reid (1961), there are some important differences. The few data points used by Reid show the North Pacific subtropical gyre as a rather smooth feature. Our maps clearly indicate the presence of a north equatorial ridge, south of which the North Equatorial Current flows westward, and north of which the Subtropical Countercurrent, described by Yoshida and Kidokoro (1967), flows eastward. There is also a pronounced ridge on the right-hand side of the Kuroshio, similar to the one outlined by Defant (1941) along the right-hand side of the Gulf Stream. In fact, the north equatorial ridge and the ridge along the Kuroshio form a continuous U-shaped ridge with its opening facing east.

When viewed on synoptic maps of dynamic topography (Japanese Oceanographic Data Center, 1967, 1968, 1969) the ridge is not always continuous but consists of several sections with eddies interspersed

among them. It is likely that cyclonic eddies, separated from the Kuroshio east of Japan, travel westward along the southeastern side of the ridge into the center of the gyre, similar to the eddies of the Gulf Stream (Fuglister, 1972). This U-shaped ridge associated with the western boundary current should be an interesting and challenging subject for theoretical studies. No similar feature seems to exist in the South Pacific Ocean.

The ridge-trough system associated with the equatorial currents is very shallow, and the dynamic topography at 500 db relative to 1000 db (not shown) is essentially flat (47 ± 1 dyn-cm) in the equatorial region between 15°N and 15°S, indicating that the equatorial currents do not penetrate substantially below 500 m. In contrast, the subtropical gyres penetrate much deeper and are clearly visible on the 1000 db relative to 2000 db topography (not shown). Their centers shift poleward, as depth increases. In the North Pacific Ocean the center of the subtropical gyre is located east of Formosa and is a rather broad feature at the sea surface. At 500 and 1000 db, the center has shifted to the area southeast of Tokyo. In the South Pacific Ocean, the center of the subtropical gyre is even broader; it extends from the Solomon Islands to Tahiti. At 500 db the eddy is more concentrated and is located east of Australia at 25°S to 30°. At 1000 db relative to 2000 db the gyre is split into two parts, the weaker off Sydney, the stronger east of New Zealand. The poleward shift of the centers of the subtropical gyres has recently been discussed by Reid and Arthur (1975). Further analysis and theoretical work on this shift might give a clue to a more suitable choice of a reference surface of variable depth, but such a study would require an analysis based on carefully selected stations, as done by Defant (1941) for the Atlantic Ocean, rather than a statistical treatment of all data.

In Antarctic waters the dynamic topography of the sea surface relative to 1000 db gives only a portion of the flow; in fact, the drop of dynamic topography across the Antarctic Circumpolar Current is 35 dyn-cm in the 1000 to 2000 m layer and 15 dyn-cm in the 2000 to 3000 m layer.

4. The mean annual variation of dynamic topography

The annual cycle of heat storage in the ocean associated with the seasonal heating and cooling is one of the major contributors to the annual changes of dynamic topography because it directly affects density. In some parts of the oceans, especially in the subpolar gyres and in parts of the tropical areas where annual salinity variations are large, salinity can also be a contributing factor. Less obvious is the role of the changing wind field in producing annual changes in dynamic topography. The wind by means of the wind stress curl and Ekman pumping can change the temperature and density structure and thereby alter the dynamic topography and the associated geostrophic flow patterns. Recently, Meyers (1975) has investigated the variations of the thermal structure during 16 consecutive monthly cruises in the trade wind region south of Hawaii and found that vertical displacements of the thermocline and associated changes in zonal geostrophic flow of the North Equatorial Current are due to Ekman pumping as related to the wind stress curl.

To illustrate mean annual changes, the surface dynamic topography relative to 1000 db is shown for the two periods March–April and November–December (Figs. 2 and 3), which exhibit maximal departures in the equatorial region. In November–December the currents north of the equator are strongest and the isopleths are more zonal than in March–April. South of the equator the situation is reversed. This agrees with tha results derived by Wyrtki (1974b) from sea level observations. Since temperature in the surface layer of the tropical ocean changes little, the changes in dynamic topography must be due to changes in the thickness of the warm upper layer, which are most likely the result of vertical displacements of the thermocline by the changing wind fields rather than the result of heating and cooling.

The transport of the North Equatorial Current always increases from east to west. It is strongest in September–October, when a dynamic height difference of 40 dyn-cm and more exists between ridge and trough everywhere from 150°W to 130°E. In January–February the difference decreases rapidly, first in the eastern and central Pacific, and later in the western Pacific, reaching minimum values of about 23 dyn-cm in March–April. This is in agreement with the annual cycle of the strength of the North Equatorial Current derived from sea level observations by Wyrtki (1974a).

The Countercurrent trough near 10°N also varies substantially during the year. It is deepest in November–December and shallowest from March to June. The equatorial ridge near 4°N is strongest and extends farthest east in November–December, but in the western Pacific it remains above 180 dyn-cm throughout the year. Annual variation of the Countercurrent determined by the slope of dynamic height between the Countercurrent trough and the equatorial ridge is somewhat different from that of the North Equatorial Current. It is weakest from March to June and strongest in November–December, in accordance with the Countercurrent trough. Its strength varies also in the east-west direction. From July to December it is stronger in the area south of Hawaii than in the western Pacific, while in January–February it is strongest in the west and decreases eastward. Wyrtki and Kendall (1967) and Wyrtki (1974b) have shown that this mean annual signal is severely masked by irregular fluctuation of the Countercurrent transport.

The western terminus of the Countercurrent trough is the Mindanao eddy, characterized by a strong low in dynamic topography. This low is most pronounced

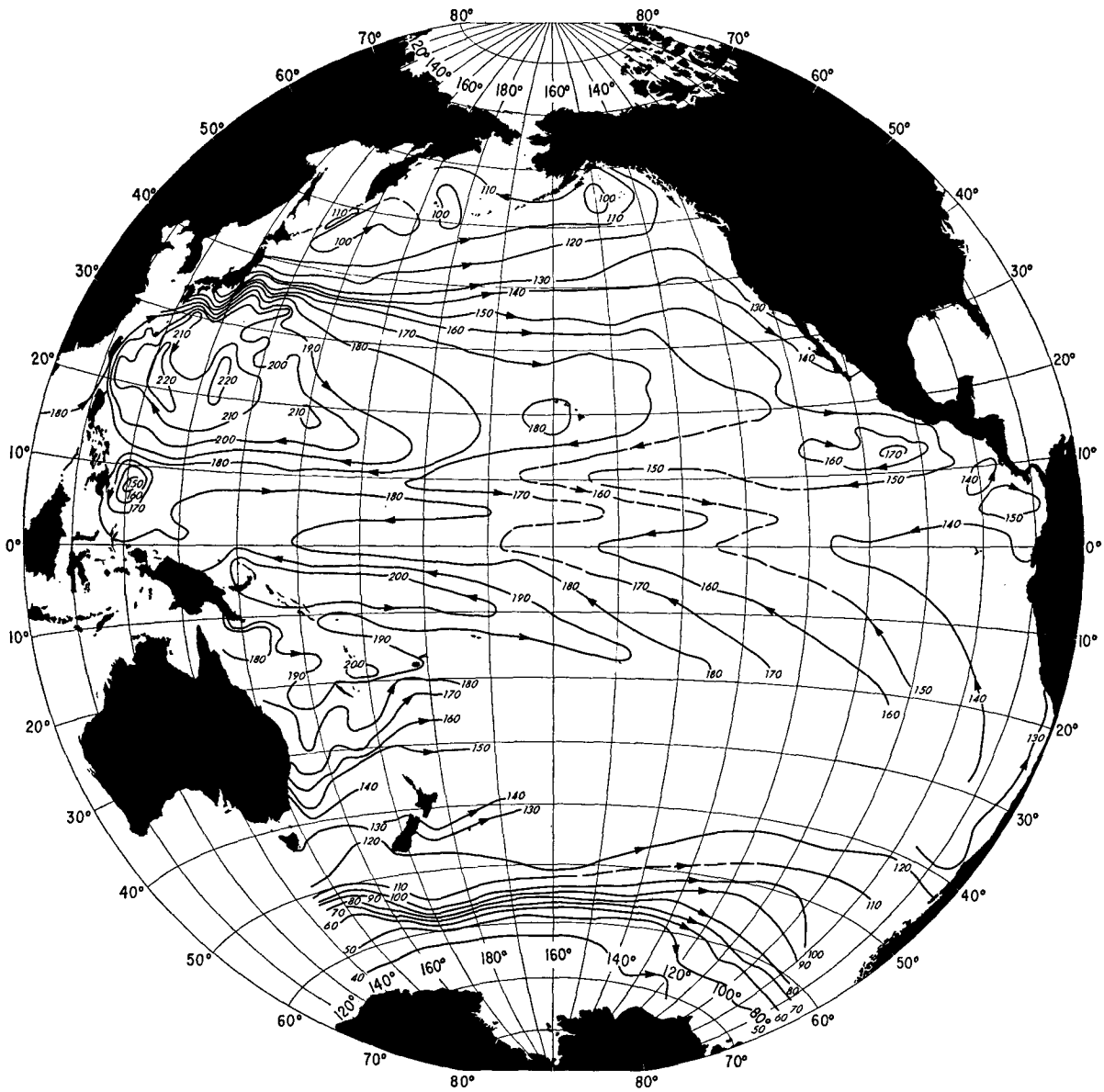

FIG. 2. Mean dynamic topography (dyn-cm) of the sea surface relative to 1000 db for the period March–April: 5,742 observations.

from March to June, when the Countercurrent is weakest and large amounts of water are recirculated between Countercurrent and North Equatorial Current. During the second part of the year, when both currents are strong, this low is not as pronounced.

Along the equator, between 100°W and 180°, an east-west slope of about 40 dyn-cm is always present, as shown by Knauss (1963). The fact that this slope is slightly stronger in the second half of the year than in the first half compares favorably with sea level records at Canton Island and the Galapagos Islands being opposite in phase. It indicates that the annual variation of the east-west slope along the equator is in opposition to the transports of the Equatorial Undercurrent, the latter documented by Taft and Jones (1973).

The subtropical anticyclonic gyre of the North Pacific undergoes considerable fluctuation during the year. Highest dynamic heights are always found east of Taiwan, but the intensity of the high relative to 1000 db varies from 216 dyn-cm in January–February to 234 dyn-cm in July–August. This variation corresponds closely to that of surface layer temperature, so one can conclude that the annual variation of dynamic height in the subtropical gyre is due to the variation of density in the surface layer as associated with variations of heat content.

The north equatorial ridge stretches across the Pacific

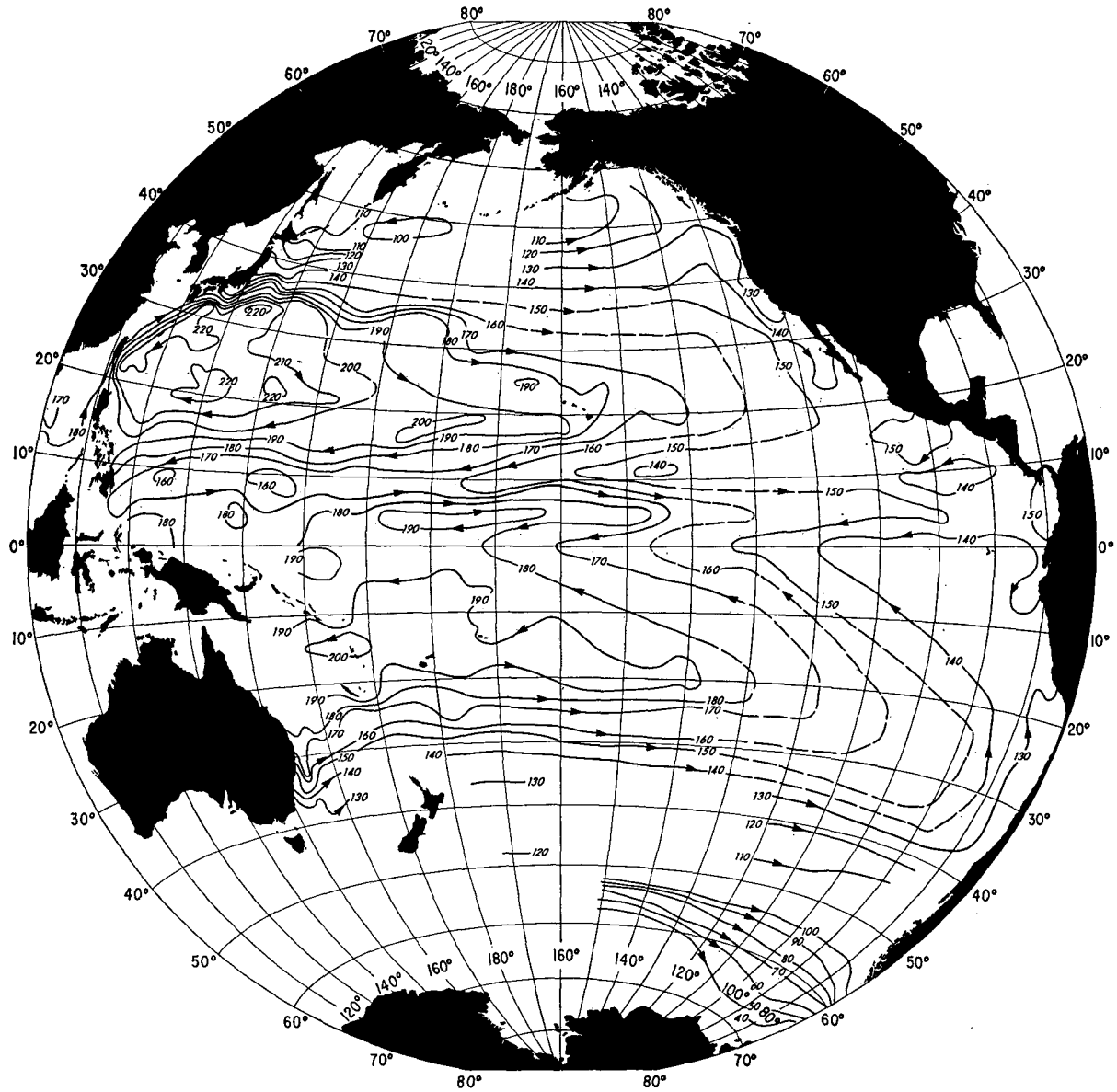

FIG. 3. Mean dynamic topography (dyn-cm) of the sea surface relative to 1000 db for the period November–December: 4,060 observations.

from the area east of Luzon past the Hawaiian Islands to about 120°W, and from March to June it penetrates into the eastern tropical Pacific. The ridge is situated slightly north of 20°N, except during the period from March to June when it is south of 20°N. Fluctuations of the subtropical high are also evident in the eastward penetration of the 190 dyn-cm isobar.

Throughout the North Pacific Current, the pattern of dynamic topography changes little during the year, although absolute values of dynamic topography increase from winter to summer by about 12 dyn-cm in the western part of the current and by about 7 dyn-cm in the eastern North Pacific. No mean annual variation of the slope across the North Pacific Current could be conclusively detected from these maps.

In the subarctic region of the Pacific the existence of two gyres, the Alaska gyre and the Kamchatka gyre, is clearly evident. It is also weakly indicated in the map by Reid (1961). Both gyres exist throughout the year. They penetrate well below 500 m depth, which is apparent from the topography of the 500 db surface relative to 1000 db. The Alaska gyre is most intense during the first half of the year and is weakest in November and December. The Kamchatka gyre seems to be weakest during the summer from June to October and strongest at the end of winter in March and April.

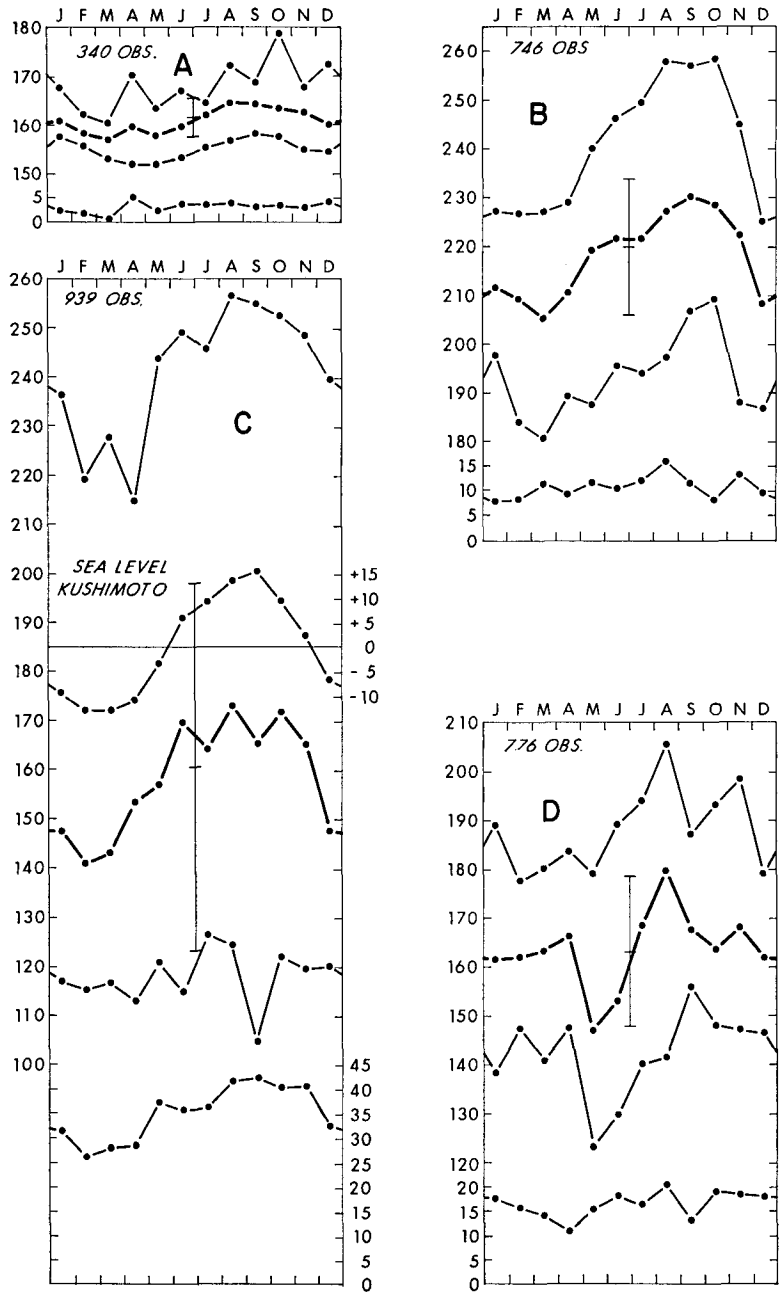

FIG. 4. Seasonal variability of dynamic height of the sea surface relative to 1000 db at ocean station *November* at 30°N, 140°W (A), south of Japan at 29°N, 135°E (B), in the Kuroshio at 33°N, 137°E (C), and at ocean station *Victor* at 34°N, 164°E (D). Shown is the mean monthly dynamic height (heavy curve), maximum and minimum values (lighter curves) and the standard deviation (bottom curve). The vertical bar gives the mean value of dynamic height and the overall standard deviation.

The subtropical anticyclonic gyre of the South Pacific Ocean also varies throughout the year, but we can make only tentative statements about the annual cycle because the density of data in our maps is rather low for the ocean south of the equator. Location, shape and intensity of the high vary substantially. It is situated between the Solomon Islands and Samoa, and is not close to the western boundary. This is probably due to the wind field in the western Pacific, which is characterized by monsoon winds during southern summer in the region between New Guinea and Fiji. During this period, from December to April, the South Equatorial Countercurrent flows east. The mean maps presented here do not show this Countercurrent in the eastern Pacific at 10°S–12°S as outlined by Reid (1961), because the current is probably highly variable in location

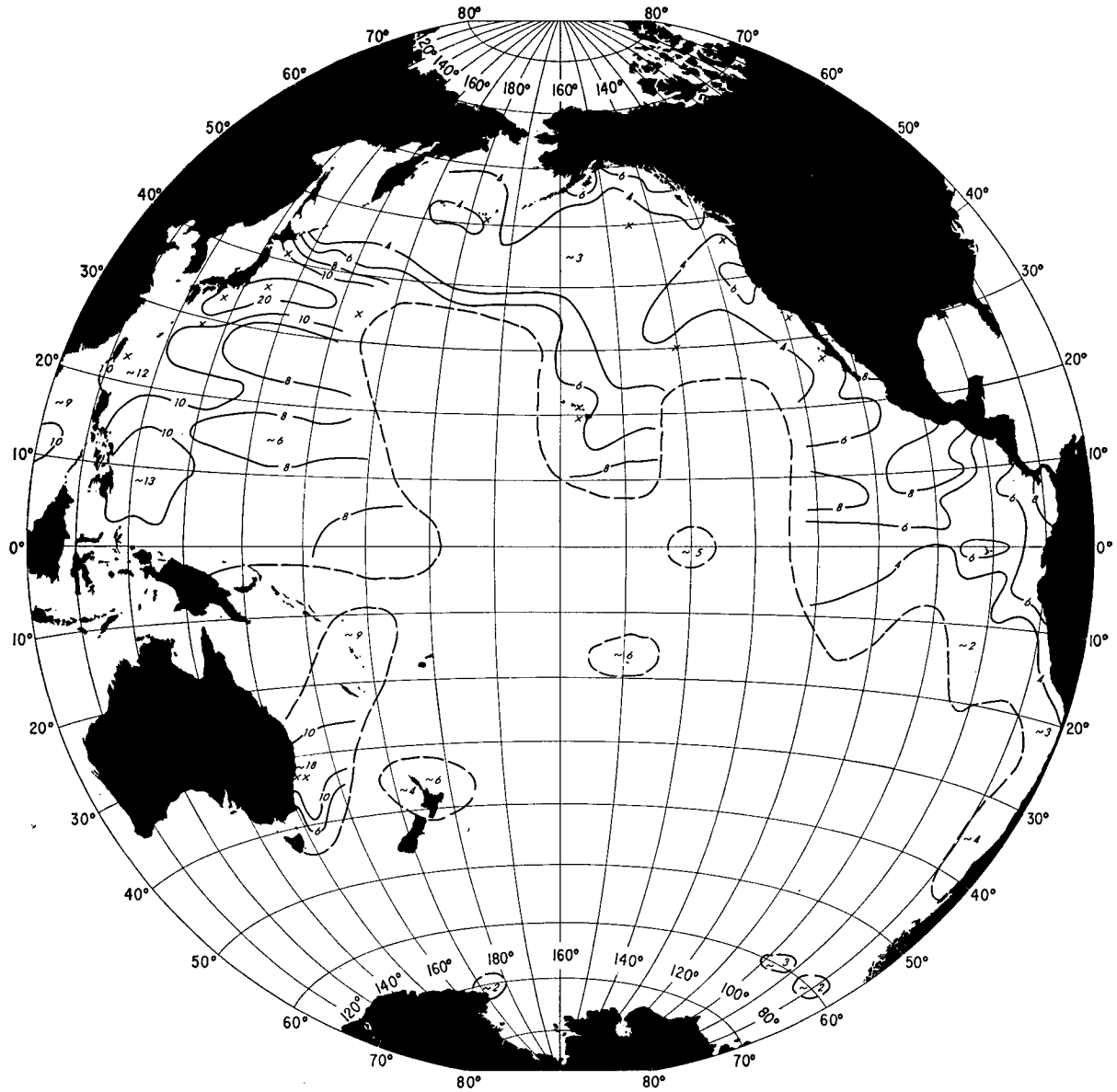

FIG. 5. Standard deviation of dynamic height (dyn-cm) of the sea surface relative to 500 db, computed irrespective of season for each 2° square having at least ten observations. Crosses indicate the positions for which data are shown in Table 1.

and chiefly below the sea surface. The subtropical high extends to the east as the south equatorial ridge and terminates at about 30°S off the coast of Chile. Nothing can be said about its variations in the eastern South Pacific because of lack of data. The pattern of dynamic topography associated with the East Australia Current differs considerably from that of the Kuroshio, but does not appear to change throughout the year. An annual cycle due to heating and cooling is apparent.

The mean annual variation of dynamic height relative to 1000 db has been analyzed at selected locations having a sufficient number of observations, usually more than 100 per 2° square. Mean dynamic heights, as well as the standard deviations, were computed for each month and are shown together with the maximum and minimum dynamic height in Fig. 4 for four representative locations. Also shown in the diagrams are the mean annual dynamic height and the overall standard deviation computed regardless of month. The same diagrams were prepared for all those locations marked by ×'s in Fig. 5 and are shown in a report by Wyrtki (1974c), but the results are summarized in Table 1.

The annual cycle of dynamic topography in subtropical and temperate latitudes is chiefly caused by the annual cycle of temperature in the surface layer, as shown by Pattullo *et al.* (1955), while the random fluctuations are more likely due to vertical displacements of the thermocline by eddies and internal waves.

The mean annual amplitude of surface temperature (Wyrtki, 1965) has been used to compute the amplitude of surface density and to determine the depth to which this density variation should penetrate in order to explain the mean annual amplitude of dynamic height. This depth, which may be called penetration depth, is given in Table 1 together with other statistical parameters. When determining density from temperature, the mean surface salinity was used, since salinity does not vary much in most regions. The rather modest values of penetration depth (50 to 125 m) indicate that the annual cycle of temperature in the upper ocean essentially determines the annual cycle of dynamic height.

At ocean station *November* (30°N, 140°W) conditions are rather quiet (Fig. 4a). The total range of dynamic height is only 33 dyn-cm, and the overall standard deviation is only 4 dyn-cm. A clear annual signal with an amplitude of 4 dyn-cm is present and most of the overall standard deviation is due to the annual cycle. The amplitude of the annual cycle can be explained by assuming that a surface layer of only 55 m thickness follows the annual surface temperature cycle. A similar situation is found along the coast of California and throughout most of the eastern parts of the subtropical gyre, as seen in Table 1.

South of Japan in the topographic high on the right-hand side of the Kuroshio, at 29°N, 135°E, the overall variability of dynamic height is 14 dyn-cm (Fig. 4b) and the total range 77 dyn-cm. An annual signal with an amplitude of 12 dyn-cm is clearly apparent, with highest dynamic heights coinciding with maximum surface temperatures in September. This annual cycle can be explained by a penetration of the surface temperature cycle to 85 m depth.

In the Kuroshio, in the 2° square centered at 33°N, 137°E, variability is extreme (Fig. 4c). Dynamic topography relative to 1000 db has a range of 150 dyn-cm; the overall standard deviation is 38 dyn-cm, and the standard deviation in individual months is equally high. This high variability is chiefly due to fluctuations in the position of the current, meanders and eddies. Moreover, the data have been averaged over a 2° square, having dimensions of roughly 200 km, while the total drop of dynamic height across the Kuroshio may take place over a distance of less than 100 km. Consequently, the presence of large horizontal gradients introduces an additional variability in the averaged data. It should also be noted that the maxima of dynamic height deviate much more from the mean curve than do the minima, indicating that the high on the right-hand side of the current only occasionally moves as close to the shore as 32°N. For comparison, the variation of sea level at Kushimoto (33°28′N, 135°47′E) is shown in Fig. 4c, and it parallels the mean monthly dynamic topography both in amplitude (14 cm) and phase.

Ocean station *Victor* (34°N, 164°E) is located in the western part of the North Pacific Current, where conditions are much more variable (Fig. 4d) than at ocean station *November* situated in the eastern part of the gyre. The range of dynamic height is 80 dyn-cm and the overall standard deviation 15 dyn-cm; both are high because of meandering of the current and the presence of eddies, but are not as extreme as in the Kuroshio south of Japan and in the Kuroshio frontal zone east of Japan (Table 1). An annual signal is apparent, but even with 776 observations it is not as regular as the annual signal at the other locations. Dynamic heights are highest in August in correspondence with the temperature cycle, and they decrease to

TABLE 1. Variability of surface dynamic height relative to 1000 db at selected locations. Values in dyn-cm.*

Location	Position		Range	Annual amplitude	Overall standard deviation	Range of monthly standard deviations	Penetration depth (m)
Ocean station *November*	30°N	140°W	33	4.0	4.2	3–4	55
Ocean station *Papa*	50°N	145°W	31	3.5	3.9	3–4	50
Ocean station *Victor*	34°N	164°E	81	(16.0)	15.4	13–18	(45)
Off California Peninsula	27°N	125°W	23	3.5	5.2	3–6	50
Off San Diego	33°N	119°W	23	3.5	4.7	3–5	90
Off Oregon	45°N	127°W	26	5.0	5.0	3–5	70
Hawaii	21°N	157°W	27	6.0	5.9	6–14	100
South of Japan	29°N	135°E	77	12.0	13.8	7–15	85
Kuroshio	33°N	137°E	150	16.0	37.7	30–40	85
Kuroshio frontal zone	37°N	145°E	156	20.0	39.6	30–40	125
Kuroshio extension	39°N	153°E	96	12.5	14.3	10–18	75
Oyashio	41°N	145°E	68	13.5	11.4	5–8	60
East of Taiwan	23°N	123°E	66	9.0	14.2	10–16	80

* Parentheses indicate that the annual cycle was not clearly defined.

a minimum in January–February. From April to May dynamic height drops substantially and then rises to the August maximum, producing a rather irregular annual cycle. The drop from April to May and the subsequent rise in dynamic height cannot be explained by temperature changes and are more likely due to a seasonal shift in the axis of the current. Because of this irregular annual cycle, its amplitude cannot easily be determined and compared to the temperature cycle.

Summarizing it may be stated that the annual cycle of dynamic height is determined by the annual cycle of temperature in the surface layer in those parts of the oceans where the annual cycle is large, namely in subtropical and temperate zones. In the equatorial region the annual cycle of dynamic height seems to be chiefly determined by the rising and falling of the thermocline in relation to the shifting wind patterns.

5. The variability of dynamic topography

Dynamic height relative to a given reference level varies according to changes in the density structure, which are caused by changes in the temperature and salinity. These changes can be due to several factors. The most important are:

1) The annual variation of the thermal structure, including the salinity structure in some regions.
2) The seasonal shift of current systems.
3) Long-term variations of density structure and circulation.
4) The meandering of currents.
5) The presence of eddies.
6) The presence of internal waves or tides.
7) The presence of large horizontal gradients in dynamic height, if data have to be averaged over a given area to draw a statistically representative sample.

All these changes are not necessarily independent of each other.

The standard deviation of surface dynamic height relative to 500 db was computed for each 2° square in the Pacific Ocean for which at least ten observations were available (Fig. 5). The 500 db reference level was chosen to make use of as many oceanographic stations as possible, and because most of the variability is contained in the upper part of the ocean. The data coverage, although sufficient only in parts of the ocean, is adequate to outline the general tendency of the distribution of variability. Unfortunately, standard deviations of dynamic height computed for larger areas [for example, 10° squares (in order to lump together a larger number of observations)] cannot be used in conjunction with the standard deviations for 2° squares, because horizontal gradients in the mean dynamic topography add variability to the computed values.

Variability is largest in the area of the Kuroshio and its extension, with a standard deviation of 25 dyn-cm. It is smallest in the subpolar gyre of the North Pacific and in the area between California and Hawaii, with a standard deviation of around 3 dyn-cm. Variability generally increases toward the coast, as in the Gulf of Alaska and off California. In the subtropical gyre it is high along the North Equatorial Ridge but decreases from west to east. Variability is strong in the region east of Mindanao where the North Equatorial Current splits, with its larger part turning north and the remainder turning south into the Mindanao Current. In the equatorial area, variability is also comparatively high, especially along the Countercurrent.

A corresponding distribution seems to prevail in the South Pacific Ocean, insofar as can be determined from areas with sufficient data. Variability is large in the East Australia Current (18 dyn-cm), but not as large as in the Kuroshio. It decreases eastward across the ocean to values of about 3 dyn-cm off South America. A few 2° squares in Antarctic waters give a surprisingly low standard deviation, but any inference from this should await the accumulation of more data.

The distribution of the variability of dynamic height as pictured in Fig. 5 clearly demonstrates that variability is largest in the western boundary currents, where the contribution from the meandering of these currents and from eddies exceeds the contribution of the annual cycle. Variability is also large in the entire western portion of the ocean and in the equatorial region, characterizing these regions as particularly active. In the subpolar and eastern parts of the oceans variability is small, indicating that eddy activity is much weaker there. In fact, standard deviations of dynamic height in the eastern parts of the ocean are as small as the errors usually attributed to the calculation of dynamic height, namely ± 2 to ± 5 dyn-cm (Stommel, 1947; Reid, 1959). Since some natural variability is certainly present even in the eastern parts of the ocean, one must conclude that the errors associated with the dynamic method are in fact smaller than those quoted.

The standard deviation of dynamic heights for individual months, shown in Fig. 4 at four locations and given as a range in Table 1, is usually somewhat smaller than the overall standard deviation to which the mean annual cycle contributes considerably. It is therefore a better measure of the activity of eddies, meanders and internal waves, than the overall standard deviation.

Acknowledgments. The author wishes to thank the National Oceanographic Data Center for providing the data on dynamic height used in this study and Mrs. Shikiko Nakahara for writing the computer programs. This research was supported by the National Science Foundation and the Office of Naval Research under the North Pacific Experiment of the International Decade of Ocean Exploration. This support is gratefully acknowledged.

REFERENCES

Defant, A., 1941: Die absolute Topographie des physikalichen Meeresniveaus und der Druckflächen, sowie die Wasserbewegungen im Atlantic Ozean. *"Meteor" Werk*, Vol. 6, No. 2, 191–260.

Emery, W. J., 1975: Dynamic height from temperature profiles. *J. Phys. Oceanogr.*, **5**, 369–375.

Fuglister, F. C., 1972: Cyclonic rings formed by the Gulf Stream 1965–66. *Studies in Physical Oceanography*, Vol. 1, A. S. Gordon, Ed., New York, Gordon and Breach, 137–168.

Japanese Oceanographic Data Center, 1967, 1968, 1969: *Kuroshio Atlas*, Vols. 1–3. Tokyo.

Knauss, J. A., 1963: The equatorial current systems. *The Sea*, Vol. 1, M. N. Hill, Ed., Interscience, 554 pp.

Meyers, G., 1975: Seasonal variation in transport of the Pacific North Equatorial Current relation to the wind field. *J. Phys. Oceanogr.*, **5**, 442–449.

National Oceanic and Atmospheric Administration, 1974: *User's Guide to NODC's Data Services*. Environmental Data Service, Washington, D. C.

Pattullo, J., W. Munk, R. Revelle and E. Strong, 1955: The seasonal oscillation in sea level. *J. Marine Res.*, **14**, 88–155.

Reid, J. L., Jr., 1961: On the geostrophic flow at the surface of the Pacific Ocean with respect to the 1,000-decibar surface. *Tellus*, **13**, 489–502.

——, and R. S. Arthur, 1975: Interpretation of maps of geopotential anomaly for the deep Pacific Ocean. *J. Marine Res.* (in press).

Reid, R. O., 1959: Influence of some errors in the equation of state or in observations on geostrophic currents. *Physical and Chemical Properties of Sea Water*, Nat. Acad. Sci., Publ. No. 600, 367–385.

Stommel, H. S., 1947: Note on the use of the *T-S* correlation for dynamic height anomaly computations. *J. Marine Res.*, **5**, 85–92.

Taft, B., and J. Jones, 1973: Measurements of the Equatorial Undercurrent in the Eastern Pacific. *Progress in Oceanography*, Vol. 6, Pergamon Press, 47–110.

Tsuchiya, M., 1974: Variation of the surface geostrophic flow in the Eastern Intertropical Pacific Ocean. *Fish. Bull.*, **72**, 1075–1086.

Wyrtki, K., 1965: The annual and semiannual variation of sea surface temperature in the North Pacific Ocean. *Limnol. Oceanogr.*, **10**, 307–313.

——, 1974a: Sea level and the seasonal fluctuations of the equatorial currents in the western Pacific Ocean. *J. Phys. Oceanogr.*, **4**, 91–103.

——, 1974b: Equatorial currents in the Pacific 1950 to 1970 and their relations to the trade winds. *J. Phys. Oceanogr.*, **4**, 372–380.

——, 1974c: The dynamic topography of the Pacific Ocean and its fluctuations. Hawaii Institute of Geophysics HIG-74-5.

——, and R. Kendall, 1967: Transports of the Pacific Equatorial Countercurrent. *J. Geophys. Res.*, **72**, 2073–2076.

Yoshida, K., and T. Kidokoro, 1967: A subtropical countercurrent (II)—A prediction of eastward flows at lower subtropical latitudes. *J. Oceanogr. Soc.* Japan, **23**, 231–246.